

1 **Loss of Dnajc21 leads to cytopenia and altered nucleotide metabolism in zebrafish**

2

3 Sarada Ketharnathan,¹ Sujata Pokharel¹, Sergey V. Prykhozhiy,¹ Anna Cordeiro-Santanach,²

4 Kevin Ban,¹ Serkan Dogan¹, Huy-Dung Hoang,^{1,3} Mira F. Liebman,^{4,5} Elaine Leung,⁵

5 Tommy Alain,^{1,3} Irina Alecu³, Steffany A.L. Bennett³, Miroslava Čuperlović-Culf,^{3,6} Yigal

6 Dror,^{7,8} Jason N Berman^{1,4}

7

8 **Supplementary Information**

9 **Contents:**

10 Supplementary Materials and Methods

11 Supplementary Figures 1-10

12 Supplementary Tables 1-2

13

14 **Supplementary Materials and Methods**

15 **Immunofluorescence assays**

16 pH3, γ -H2AX and Dnajc21 staining was performed as previously described (1). Embryos were

17 blocked using 2% sheep serum (Millipore Sigma) and 1% bovine serum albumin (Wisent,

18 Saint-Jean-Baptiste, Canada) followed by incubation with rabbit anti-pH3 antibody (06-570,

19 Millipore Sigma, 1:500), rabbit anti-DNAJC21 antibody (23411-1-AP, Thermo Fisher, 1:200)

20 or rabbit anti- γ -H2A.X (ab228655, abcam, Cambridge, UK, 1:300) at 4°C. The secondary

21 antibodies used were AlexaFluor488-conjugated goat anti-rabbit antibody (A-11008, Thermo

22 Fisher, 1:750) or AlexaFluor647-conjugated donkey anti-rabbit antibody (A-31573, Thermo

23 Fisher, 1:500). For apoptosis detection, live embryos were stained with 10 μ g/mL acridine

24 orange (Millipore Sigma) at 28°C for 30 minutes. Stained embryos were imaged on a Zeiss

25 Axiozoom.V16 stereomicroscope and GFP⁺ cells were counted using the Cell Counter plugin
26 on ImageJ (2).

27

28 **Quantitative PCR and RNA sequencing**

29 Total mRNA was extracted from pools of 30 embryos or kidney marrow from single fish using
30 Trizol (Thermo Fisher) according to the manufacturer's instructions. Complementary DNA
31 was synthesized using M-MuLV Reverse Transcriptase (New England Biolabs, Ipswich, MA,
32 USA) and Random Primer 9 (New England Biolabs). qPCR was performed using BlasTaq™
33 Probe 2X qPCR MasterMix (Applied Biological Materials) on a BioRad CFX96 Realtime PCR
34 machine. Reference genes used were *actb1* and *eef1a11l*.

35 For RNA sequencing, libraries were prepared using the Illumina Stranded Total RNA Prep kit.
36 150 bp paired-end sequencing was performed on the Illumina Next Seq 500 platform.
37 Approximately 16 million reads were obtained per sample. Reads were aligned to the zebrafish
38 GRCz11 reference genome using the STAR algorithm (3) followed by gene and transcript
39 quantification using the zebrafish transcriptome annotation published by Lawson *et al* (4).
40 Differentially expressed genes were identified using edgeR (5) and gene ontology enrichment
41 of biological processes was performed using FishEnrichr (6).

42

43 **Cell cycle analysis**

44 Zebrafish embryos untreated or treated with 100 mM thymidine were collected at 48 hpf,
45 deyolked and dissociated by incubating with collagenase (Millipore Sigma) at 37°C for 30
46 minutes. Cells were pelleted, fixed in 4% PFA and permeabilized using 10% triton X-100 and
47 5% sodium citrate. The cells were incubated with FxCycle™ Violet Stain (Thermo Fisher) for

48 30 minutes and analyzed on a Cytex Aurora cytometer (Cytex Biosciences, Fremont, CA,
49 USA). Analysis was carried out using Kaluza Analysis Software (Beckman Coulter).

50

51 **Polysome profiling and western blotting**

52 For polysome profiling, 200 larvae per sample were treated with 0.1 mg/ml cycloheximide
53 for 10 minutes and resuspended in hypotonic lysis buffer for 30 minutes, as previously
54 described (7). Lysates were loaded onto 5-25% or 10-50% linear sucrose gradients and
55 centrifuged at 36,000 rpm for 2 hr using a SW41Ti rotor. Fractionation was carried out using
56 a Brandel Fraction Collector system. For puromycin incorporation assay, larvae were treated
57 with 50 µg/mL puromycin (Millipore Sigma) for one hour, followed by lysis and western
58 blotting as described below.

59 Protein was extracted from pools of 50 embryos at 5 days post-fertilization (dpf) using RIPA
60 lysis buffer (Millipore Sigma). Proteins were resolved by SDS-polyacrylamide gel
61 electrophoresis and transferred to a nitrocellulose membrane. Following blocking with 5%
62 milk in Tris-buffered saline with Tween, membranes were incubated with primary antibody:
63 mouse anti-puromycin antibody (MABE343, Millipore Sigma, 1:1000) or rabbit anti-
64 GAPDH (ab181602, abcam, 1:10,000) antibody overnight at 4°C. The secondary antibody
65 used was goat anti-rabbit IgG HRP-linked antibody (G-21234, Thermo Fisher, 1:1000) or
66 goat anti-mouse IgG HRP-linked antibody (G-21040, Thermo Fisher, 1:1000). Signals were
67 detected using the SuperSignal™ West Atto Ultimate Sensitivity Substrate (Thermo Fisher).

68

69 **Lipopolysaccharide (LPS) and *gcsf* assays**

70 To evaluate microbial inflammatory responses, wildtype or *dnajc21*^{-/-} zebrafish embryos
71 carrying the *Tg(mpx:eGFP)* transgene at 48 hours post-fertilization were anaesthetized in

72 0.02% Tricaine and the yolk was injected with 1 mg/ml LPS (or PBS as control). Injected
73 embryos were incubated at 28°C for 4 hours before imaging. GFP⁺ cells in the yolk region
74 were counted using the Cell Counter plugin on ImageJ. For *gcsf* induction of neutrophils,
75 zebrafish embryos at the one-cell stage were injected with either 20 ng/μL or 100 ng/μL of
76 capped zebrafish *gcsf* mRNA. Embryos were fixed at 48 hpf for Sudan Black staining, as
77 detailed above.

78

79 **Metabolomics assays**

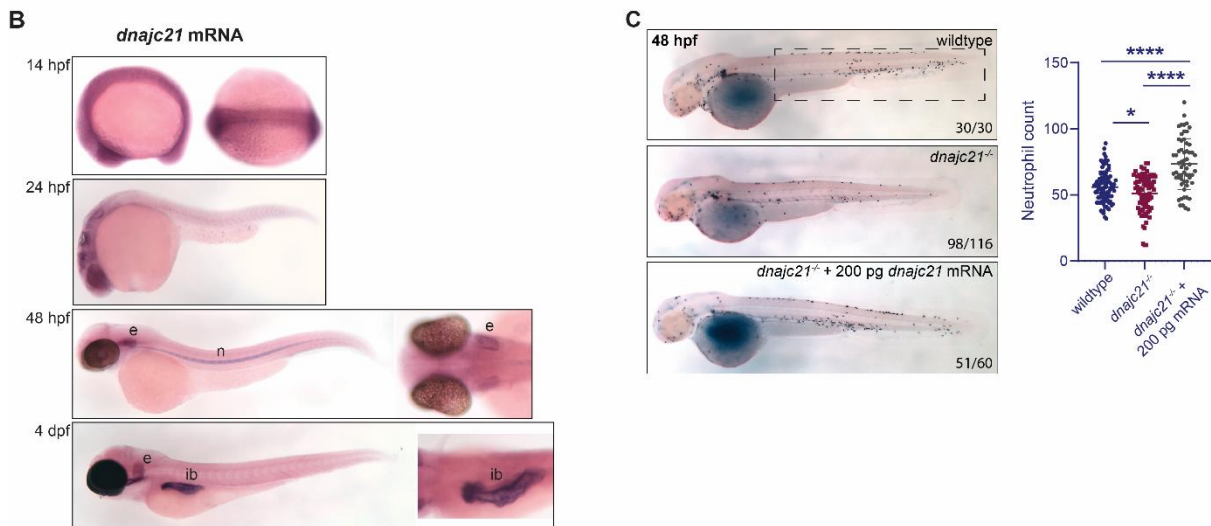
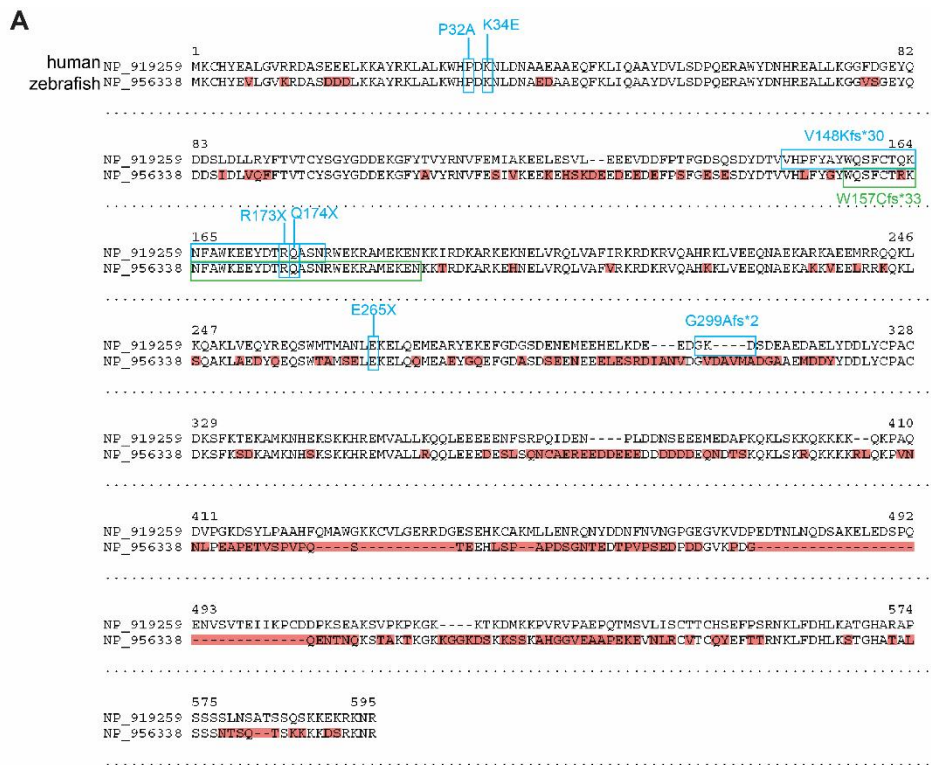
80 Each sample consisted of a pool of 60 deyolked embryos at 48 hpf or 3 whole kidney
81 marrows from fish at 8 months post-fertilization (mpf). Samples were pelleted into tubes
82 containing four washed ceramic beads (2.8 mm). Then, 1026 ul of methanol:water (1:1) was
83 added and stored at -80°C until extraction. At the time of extraction, 594 ul of acetonitrile
84 was added followed by bead beating twice at 30Hz for 2 minutes. Samples were incubated
85 with a dichloromethane:water (1:1) solution followed by centrifugation at 4000 g for 10
86 minutes at 1°C. The upper polar phase was dried using a refrigerated CentriVap Vacuum
87 Concentrator (LabConco Corporation, Kansas City, MO, USA). Samples were resuspended
88 in water and run on an Agilent 6470A tandem quadruple mass spectrometer equipped with an
89 Agilent 1290 Infinity II ultra-high performance liquid chromatography system, utilizing the
90 Metabolomics Dynamic MRM database and method (Agilent, Santa Clara, CA, USA)(8). For
91 phosphate-containing metabolites, 5 uM InfinityLab deactivator (Agilent) was added.
92 Multiple reaction monitoring (MRM) transitions were optimized using authentic standards
93 and quality control samples. Metabolites were quantified by integrating the area under the
94 curve of each compound with external standard calibration curves using the Mass Hunter
95 Quantitative analysis software (Agilent). No corrections for ion suppression or enhancement
96 were performed.

97 **Data analysis:** Hierarchical cluster analysis of metabolite concentrations was performed in
98 MetaboAnalyst 5.0(9) on \log_{10} transformed and pareto-scaled data, and is presented as
99 heatmaps. Pathway over-representation analysis of different groups of metabolites was also
100 performed using MetaboAnalyst 5.0(9) for selected lists of metabolites. Only pathways with
101 $p\text{-value} < 0.01$ are shown, where $p\text{-value}$ represents the probability of seeing the observed
102 number of metabolites in the pathway for a given input list of metabolites. Indicated in all
103 results is also the enrichment ratio, calculated as the number of hits within a particular
104 metabolic pathway divided by the expected number of hits for the background (input) set.
105 Metabolite feature selection and network analysis was performed in Matlab (Matworks Inc)
106 following metabolite autoscaling. Selection of the most significantly different metabolites
107 between wildtype and mutant groups was done using Relieff, a machine learning based
108 feature selection methods(10). Top metabolites selected by Relieff were used to explore over-
109 representation of active pathways in mutants. In this case, correlation partners for the most
110 significantly differentially concentrated features are calculated using distance correlation
111 analysis(11) with significant correlation partners selected to have $p\text{-value} < 0.01$. List of
112 correlation partners of significantly different metabolites is determined for mutant samples
113 and used to obtain pathways with strongest link to the major metabolic differences between
114 wildtype and *dnajc21* mutants.

115 Changes in relationships and activity of pyrimidine and purine pathways resulting in DNA
116 and RNA synthesis were determined through comparison of correlations between bottleneck
117 point metabolites at the intersection between *de novo* synthesis, salvage pathway and
118 downstream metabolism. Correlations were made to UMP for pyrimidine metabolism, and to
119 IMP for purine metabolism. Changes in correlations in wildtype and mutant groups are
120 indicated as metabolites that have distance correlation above 0.9 in one group and below 0.7
121 in the other group.

122 **Supplementary Figures**

123



124

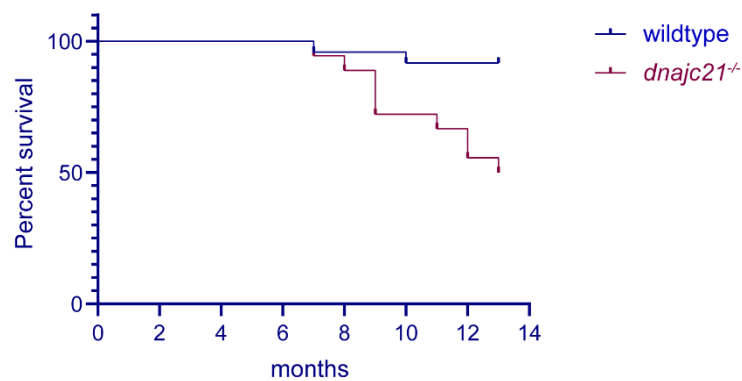
125 **Supplementary Figure 1. Characterization of *dnajc21* expression during zebrafish**
126 **embryogenesis.**

127 **A** Alignment of human and zebrafish protein using Benchling. Mismatches are highlighted in
128 orange. DNAJC21 mutations reported in SDS patients are annotated in blue. The *dnajc21*

129 mutation carried by our zebrafish line, W157Cfs*33, is annotated in green. **B** Whole-mount
130 *in situ* hybridization showing expression of *dnajc21* mRNA at 14, 24, 48 and 96 hours post-
131 fertilization (hpf). e-ear, n-notochord, ib-intestinal bulb. Two biological replicates, each
132 comprising 30 embryos, were analyzed. **C** Lateral views of Sudan Black staining in wildtype
133 uninjected, *dnajc21*^{-/-} mutants uninjected or *dnajc21*^{-/-} mutants injected with 200 pg zebrafish
134 *dnajc21* wildtype mRNA, at 48 hpf. Two biological replicates, each comprising 30 embryos
135 per condition, were analyzed. Numbers on the lower right indicate the number of larvae with
136 the representative phenotype. The black dotted box indicates the region of the embryo used
137 for counting. Number of neutrophils per embryo is quantified in the graph. hpf: hours post-
138 fertilization. *p<0.01, ****p<0.00001.

139

140

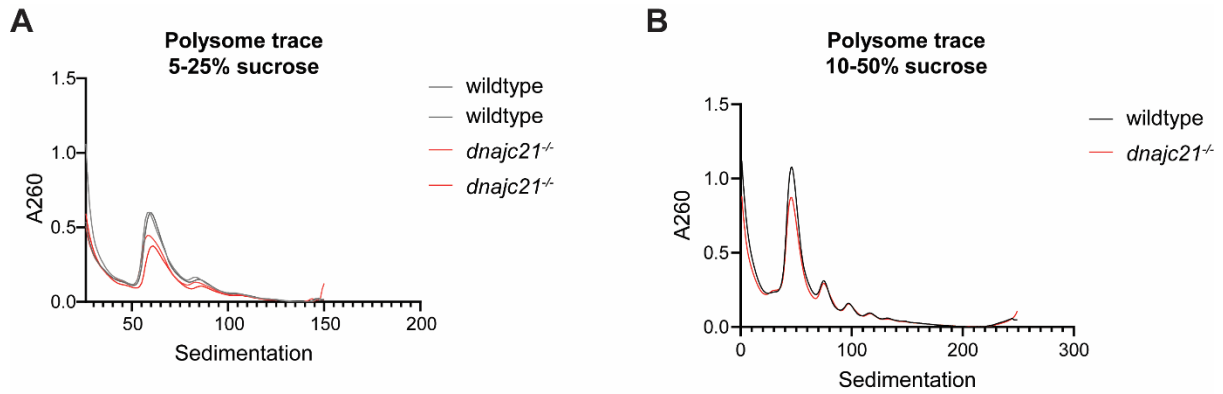


141

142 **Supplementary Figure 2. *dnajc21*^{-/-} mutants show reduced survival by 8 months of age.**

143 Kaplan-Meier survival curves for *dnajc21*^{-/-} mutant (n=18) and wildtype (n=24) fish. Log-
144 rank (Mantel-Cox) test: p=0.0029.

145



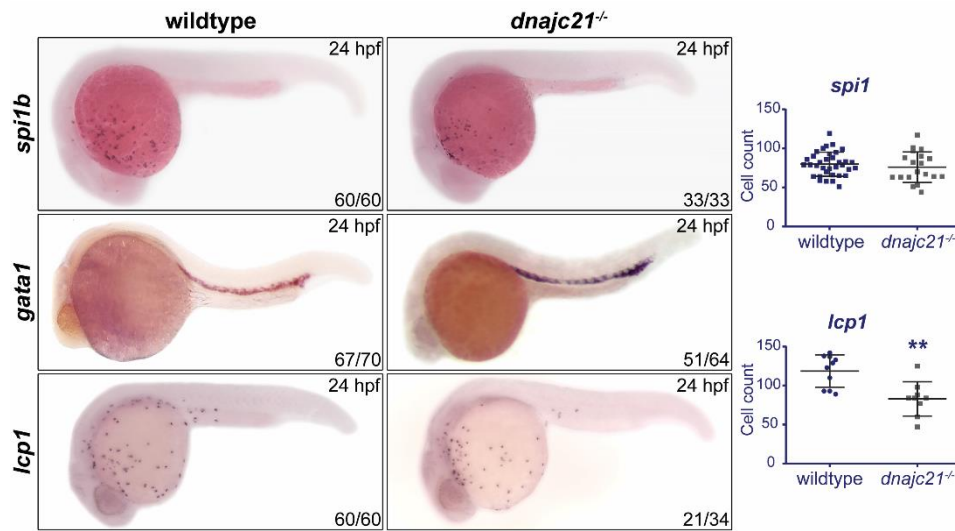
146

147 **Supplementary Figure 3. Different sucrose gradients yield similar mutant polysome**
 148 **profiles.**

149 Polysome traces generated with **A** 5-25% and **B** 10-50% sucrose gradients are shown.

150 *dnajc21* mutants have reduced 80S monosome and polysome peaks compared to wildtype
 151 embryos at 5 days post-fertilization.

152



153

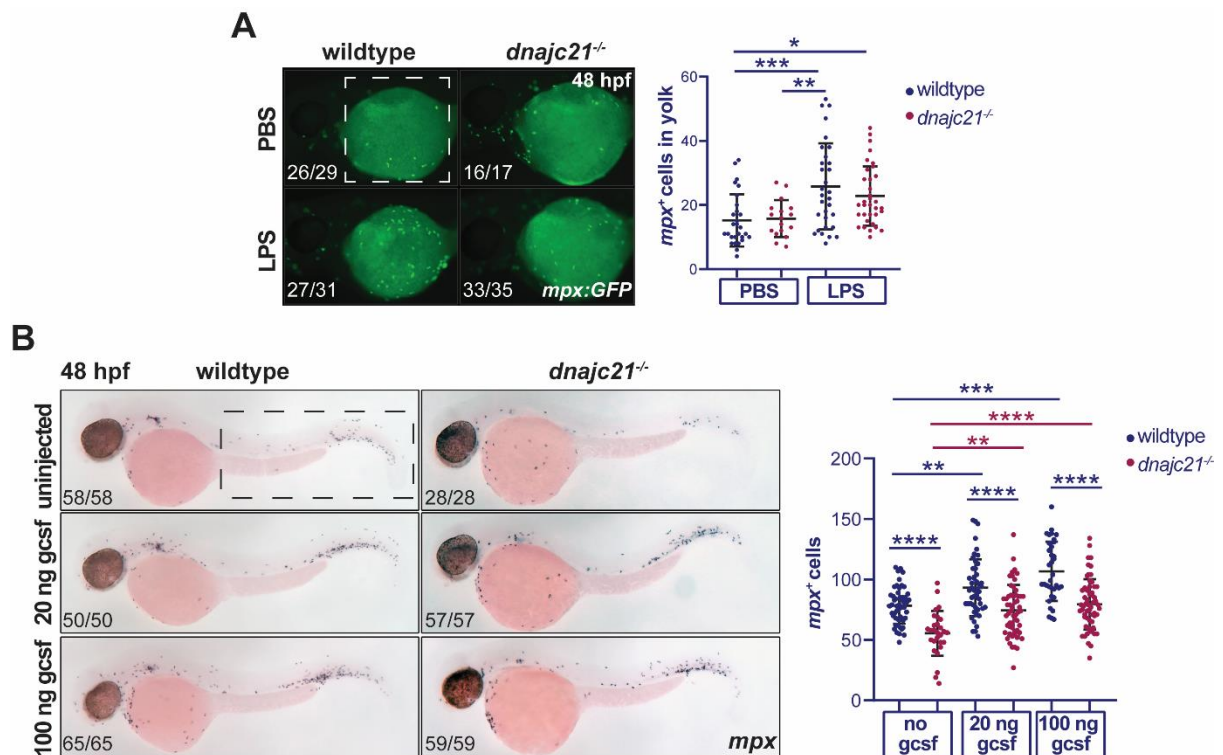
154 **Supplementary Figure 4. Expression of *gata1* and *spi1* remain normal, while *lcp1* is**
 155 **reduced during primitive hematopoiesis.**

156 Brightfield images of whole-mount *in situ* hybridization for *spi1b*⁺ myeloid progenitors,

157 *gata1*⁺ erythroid progenitors and *lcp1*⁺ total leukocytes at 24 hpf. Lateral views are shown

158 with anterior to the left. Numbers on the lower right indicate the number of embryos with the
 159 same phenotype. Experiments were done in 2 or 3 biological replicates, each comprising of at
 160 least 15 embryos per genotype. Graphs show quantification of cell counts per embryo. hpf:
 161 hours post-fertilization. ** $p < 0.001$.

162



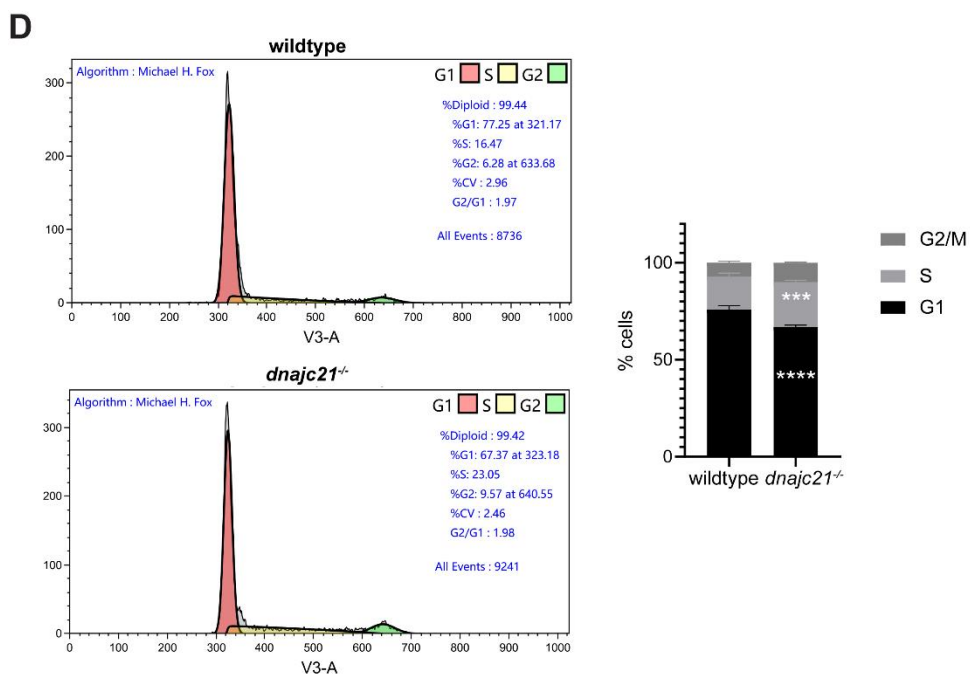
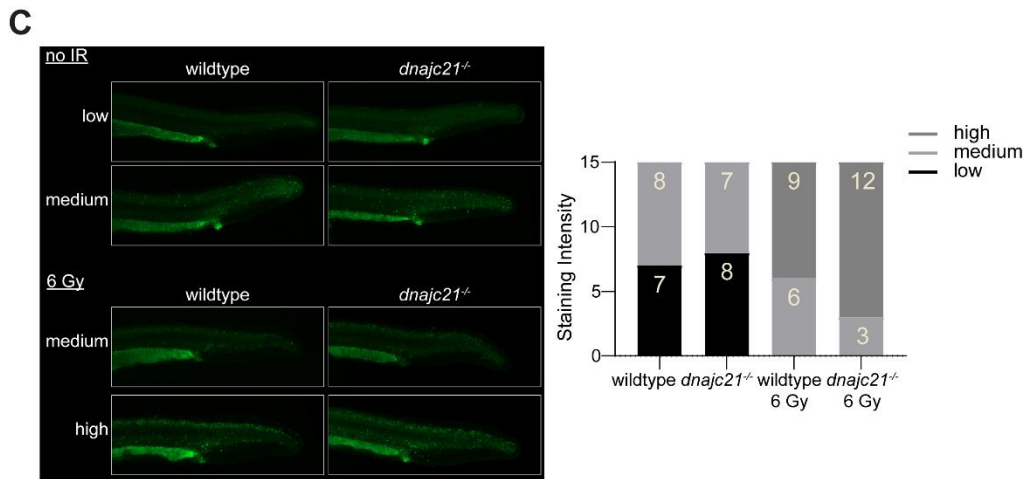
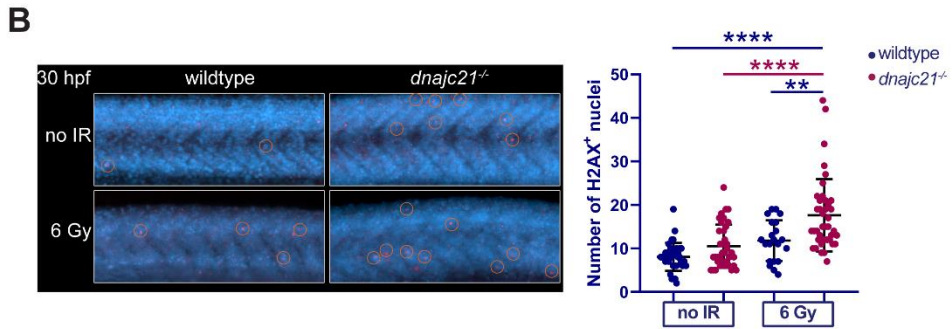
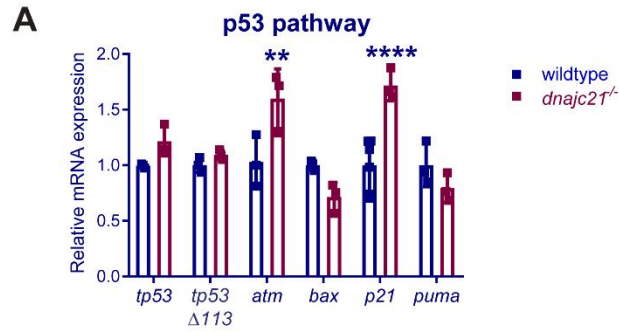
163

164 **Supplementary Figure 5. *dnajc21* mutants exhibit poor responses to LPS and *gcsf***
 165 **challenges.**

166 **A** Wildtype and *dnajc21*^{-/-} mutant fish carrying the *mpx:eGFP* transgene were generated by
 167 crossing the respective genotypes into the background of *mpx:eGFP* transgenic zebrafish.
 168 Lateral views of *Tg(mpx:eGFP)* wildtype and *dnajc21*^{-/-} embryos injected with LPS or PBS in
 169 the yolk at 48 hpf. Neutrophil recruitment was measured at 4 hours post-injection by counting
 170 the number of GFP⁺ cells in the yolk. The white dotted box marks the region used for
 171 counting. The number of neutrophils is quantified in the graph. **B** Lateral views of WISH for

172 *mpx* at 48 hpf following injections with 20 ng or 100 ng of *gcsf* mRNA at the one-cell stage.
173 The black dotted box marks the region in the trunk used for counting. The number of *mpx*⁺
174 neutrophils is quantified in the graph. Numbers on the lower left indicate the number of
175 embryos with the same phenotype. Experiments were done in 2 biological replicates, each
176 comprising of at least 20 embryos per condition. hpf: hours post-fertilization. *p<0.01;
177 **p<0.001; ***p<0.0001; ****p<0.00001.

178



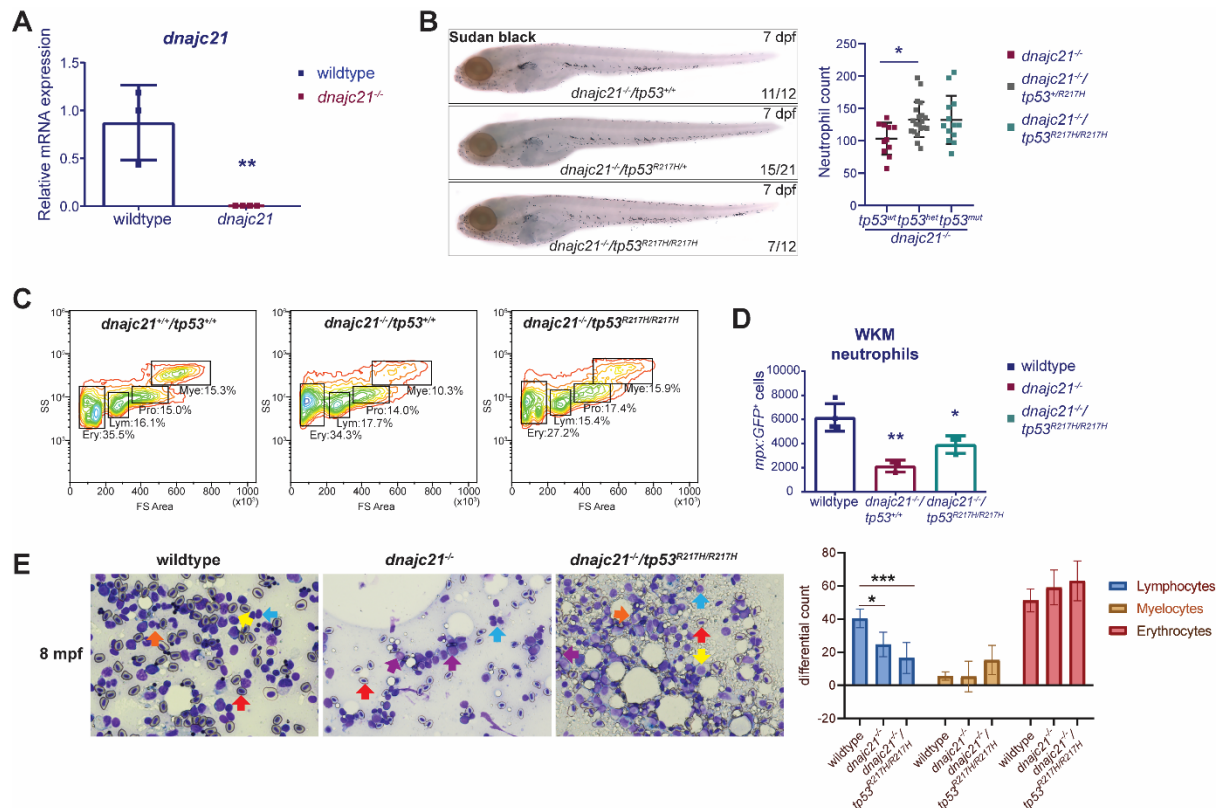
180 **Supplementary Figure 6. *dnajc21* mutants show increased DNA damage and are**
181 **sensitive to γ -irradiation.**

182 **A** Quantification of mRNA levels of *tp53* and its targets by qPCR at 48 hpf. *b-actin* and
183 *eefla111* were used for normalization. **B-C** Wildtype and *dnajc21*^{-/-} mutants were not exposed
184 (no IR) or exposed to 6 Gy γ -irradiation at 24 hpf. At 6 hours post-irradiation,
185 immunostaining for the DNA damage marker, γ -H2AX, or acridine orange staining to detect
186 apoptotic cells were performed. **B** Lateral magnified views of the embryonic trunk region
187 above the yolk extension showing γ -H2AX (red circles) and nuclei (blue). The number of γ -
188 H2AX⁺ nuclei per embryo is quantified in the graph. Two biological replicates were assayed;
189 wildtype no IR=37 embryos; wildtype 6 Gy IR=22 embryos; *dnajc21*^{-/-} no IR=37 embryos;
190 *dnajc21*^{-/-} 6 Gy IR=40 embryos. **C** Lateral views acridine orange staining in the trunks of
191 wildtype and *dnajc21*^{-/-} mutant embryos. Embryos are classified based on staining pattern as
192 low, medium or high. **D** Cell cycle analysis of embryos at 48 hpf using FxCycle™ Violet by
193 flow cytometry. Graph shows the distribution of cells in G1, S and G2/M phases. hpf: hours
194 post-fertilization. **p<0.001; ***p<0.0001 ****p<0.00001.

195

196

197



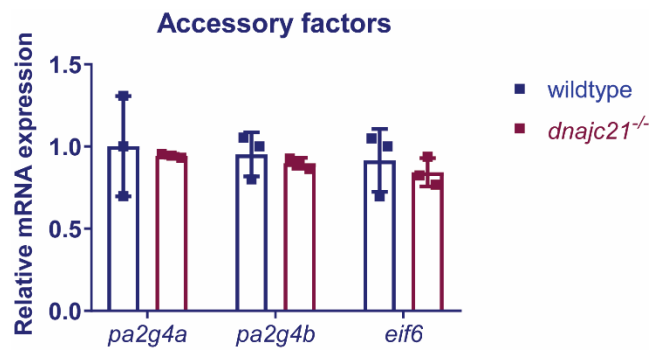
198

199 **Supplementary Figure 7. Introduction of the *tp53* R217H mutation improves neutrophil**
 200 **counts in the *dnajc21* mutants.**

201 **A** Levels of *dnajc21* mRNA in the kidney marrows of wildtype and *dnajc21* mutant fish at 8
 202 mpf, measured by qPCR. *b-actin* and *eef1a11l* were used for normalization. **B** Lateral views
 203 of Sudan Black staining in *dnajc21*^{-/-}, *dnajc21*^{-/-}/*tp53*^{R217H/+} and *dnajc21*^{-/-}/*tp53*^{R217H/R217H}
 204 mutant larvae at 7 dpf. Experiments were done in 2 biological replicates, each comprising of
 205 at least 10 embryos per genotype. Numbers on the lower right indicate the number of larvae
 206 with the same phenotype. Graph shows quantification of neutrophils per embryo. **C**
 207 Representative scatter plots showing the distribution of the four major hematopoietic
 208 populations in the kidney marrow in wildtype, *dnajc21*^{-/-} and *dnajc21*^{-/-}/*tp53*^{R217H/R217H} mutant
 209 fish at 4 mpf. Ery: erythrocytes; Lym: lymphocytes; Pro: progenitors; Mye: myelomonocytes.
 210 **D** Quantification of neutrophil counts using the *mpx:eGFP* transgenic reporter in wildtype,
 211 *dnajc21*^{-/-} and *dnajc21*^{-/-}/*tp53*^{R217H/R217H} mutant fish at 4 mpf. **E** Representative images from

212 Giemsa staining of kidney marrow touch preparations from wildtype (n=8), *dnajc21*^{-/-} (n=3)
213 and *dnajc21*^{-/-}/*tp53*^{R217H/R217H} (n=4) fish at 8 mpf. Arrows indicate mature erythrocytes (red),
214 lymphocytes (blue), myelocytes (yellow), mature neutrophils (orange) and immature
215 progenitors (purple). Differential counts for lymphocytes and myelocytes and erythrocytes
216 are shown in the graph. dpf: days post-fertilization; mpf: months post-fertilization *p<0.01;
217 **p<0.001; ***p<0.0001.

218



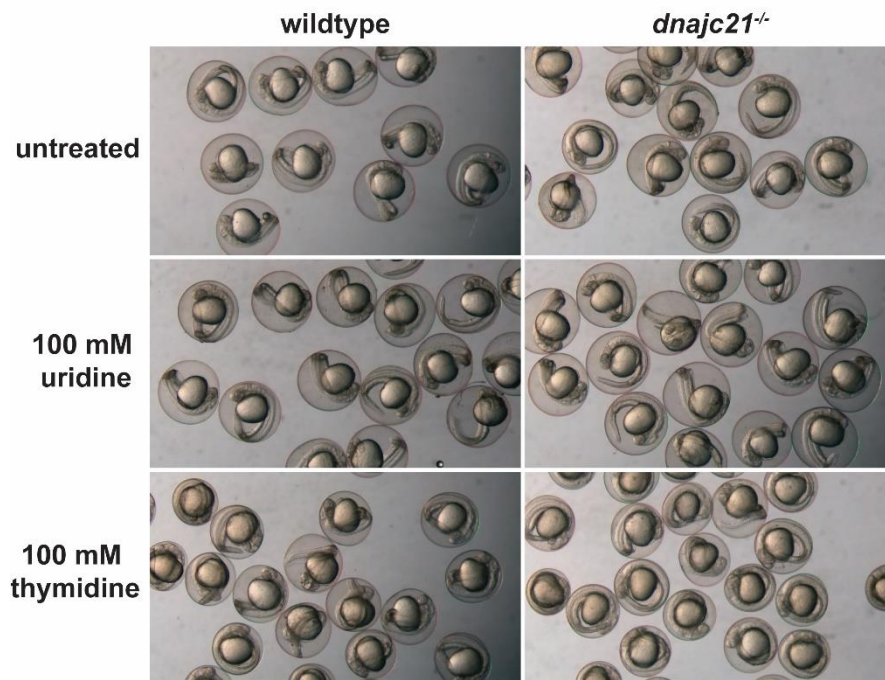
219

220 **Supplementary Figure 8. No evidence of functional compensation in *dnajc21* mutants.**

221 qPCR analysis of genes encoding accessory proteins that function together with Dnajc21 in
222 the 60S ribosomal maturation pathway. Gene expression was measured in kidney marrows
223 isolated from wildtype and *dnajc21*^{-/-} mutant fish at 8 months of age. *b-actin* and
224 *eef1a111* were used for normalization.

225

226



227

228 **Supplementary Figure 9. No toxicity was observed with nucleoside treatment.**

229 Brightfield images showing normal morphology in wildtype or *dnajc21^{-/-}* embryos treated

230 with 100 mM uridine or thymidine from 3 to 48 hpf.

231

232

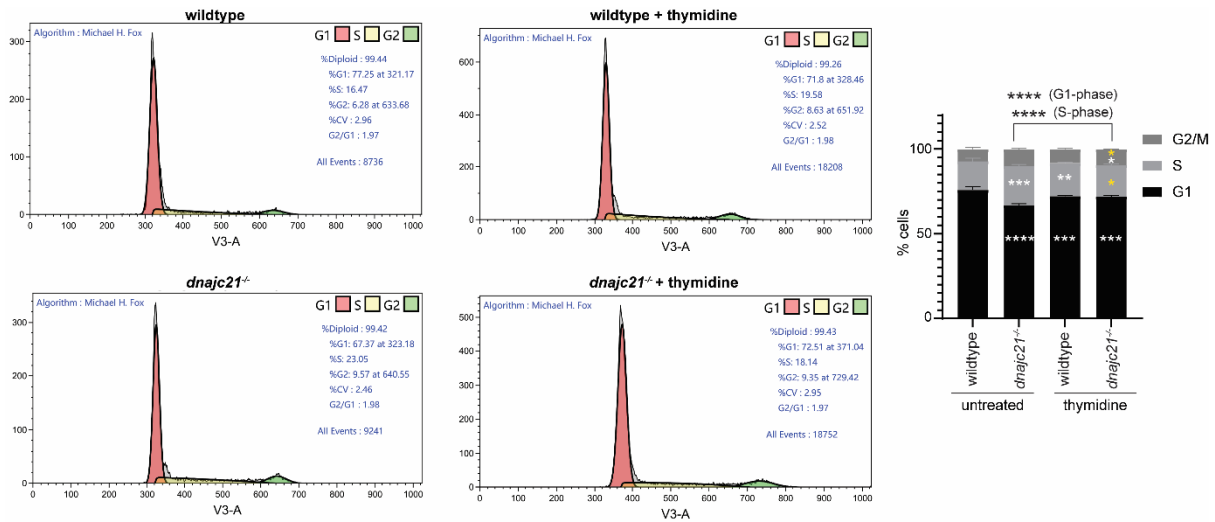
233

234

235

236

237



sgRNA	Exon location	sgRNA sequence	Direction
1	Exon 5	accgctgggagaagagag	-
2	Exon 5	agaagagagccatggaga	+
3	Exon 5	caagcgagacaagcgtgtg	-
4	Exon 5	caggctcataagaagctgg	+
5	Exon 6	atggaggctgaatatggac	+
6	Exon 6	tgaatatggacaggagtt	+

7	Exon 6	agtcgggacatagcaaag	+
---	--------	--------------------	---

248

249 **Supplementary table 2.** Concentrations of metabolites measured in embryonic and kidney
250 marrow samples from wildtype and *dnajc21*^{-/-} mutant fish. (submitted as separate file)

251

252 **Supplementary References**

- 253 1. Verduzco D, Amatruda JF. Analysis of Cell Proliferation, Senescence and Cell Death in
254 Zebrafish Embryos. *Methods Cell Biol.* 2011;101:10.1016/B978-0-12-387036-0.00002-5.
- 255 2. Schneider CA, Rasband WS, Eliceiri KW. NIH Image to ImageJ: 25 years of image
256 analysis. *Nat Methods.* 2012 Jul;9(7):671–5.
- 257 3. Dobin A, Davis CA, Schlesinger F, Drenkow J, Zaleski C, Jha S, et al. STAR: ultrafast
258 universal RNA-seq aligner. *Bioinformatics.* 2013 Jan 1;29(1):15–21.
- 259 4. Lawson ND, Li R, Shin M, Grosse A, Yukselen O, Stone OA, et al. An improved
260 zebrafish transcriptome annotation for sensitive and comprehensive detection of cell type-
261 specific genes. Stainier DY, Busch-Nentwich E, Crump G, Busch-Nentwich E, editors.
262 *eLife.* 2020 Aug 24;9:e55792.
- 263 5. Robinson MD, McCarthy DJ, Smyth GK. edgeR: a Bioconductor package for differential
264 expression analysis of digital gene expression data. *Bioinformatics.* 2010 Jan 1;26(1):139–
265 40.
- 266 6. Kuleshov MV, Jones MR, Rouillard AD, Fernandez NF, Duan Q, Wang Z, et al. Enrichr: a
267 comprehensive gene set enrichment analysis web server 2016 update. *Nucleic Acids Res.*
268 2016 Jul 8;44(W1):W90-97.
- 269 7. Gandin V, Sikström K, Alain T, Morita M, McLaughlan S, Larsson O, et al. Polysome
270 Fractionation and Analysis of Mammalian Translatomes on a Genome-wide Scale. *JoVE*
271 (Journal of Visualized Experiments). 2014 May 17;(87):e51455.
- 272 8. Sartain MJ. The Agilent Metabolomics Dynamic MRM Database and Method. 2016.
- 273 9. Pang Z, Chong J, Zhou G, de Lima Morais DA, Chang L, Barrette M, et al.
274 MetaboAnalyst 5.0: narrowing the gap between raw spectra and functional insights.
275 *Nucleic Acids Research.* 2021 Jul 2;49(W1):W388–96.
- 276 10. Urbanowicz RJ, Meeker M, La Cava W, Olson RS, Moore JH. Relief-based feature
277 selection: Introduction and review. *Journal of Biomedical Informatics.* 2018 Sep 1;85:189–
278 203.

279 11. Monti F, Stewart D, Surendra A, Alecu I, Nguyen-Tran T, Bennett SAL, et al. Signed
280 Distance Correlation (SiDCo): an online implementation of distance correlation and partial
281 distance correlation for data-driven network analysis. *Bioinformatics*. 2023 May
282 1;39(5):btad210.

283